Nature Methods

Monitoring multiple distances within a single molecule using switchable FRET

Stephan Uphoff, Seamus J Holden, Ludovic Le Reste, Javier Periz, Sebastian van de Linde, Mike Heilemann & Achillefs N Kapanidis

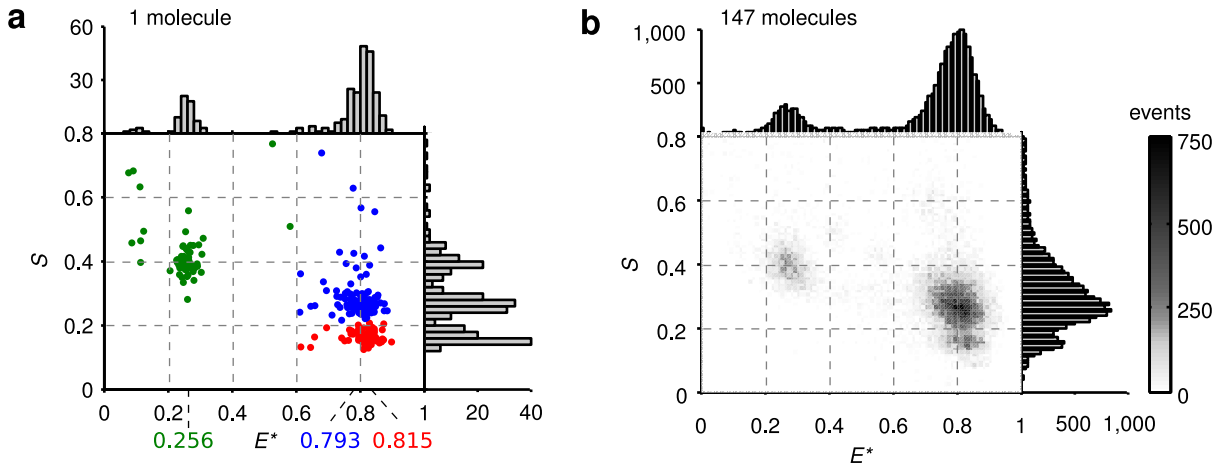

Supplementary Figure 1 | Single-molecule vs. combined E^*-S histogram for Cy5-Cy3B-Cy5 sample. (**a,b**) Single-molecule data from **Fig. 2** (mean E^* of the clusters are given below the 2D scatter plot) compared to the combined data of 147 molecules under identical conditions. The higher abundance of the 0-DA state compared to the A-D0 state is due to the higher activation rate of the proximal acceptor; the deactivation rates are similar.

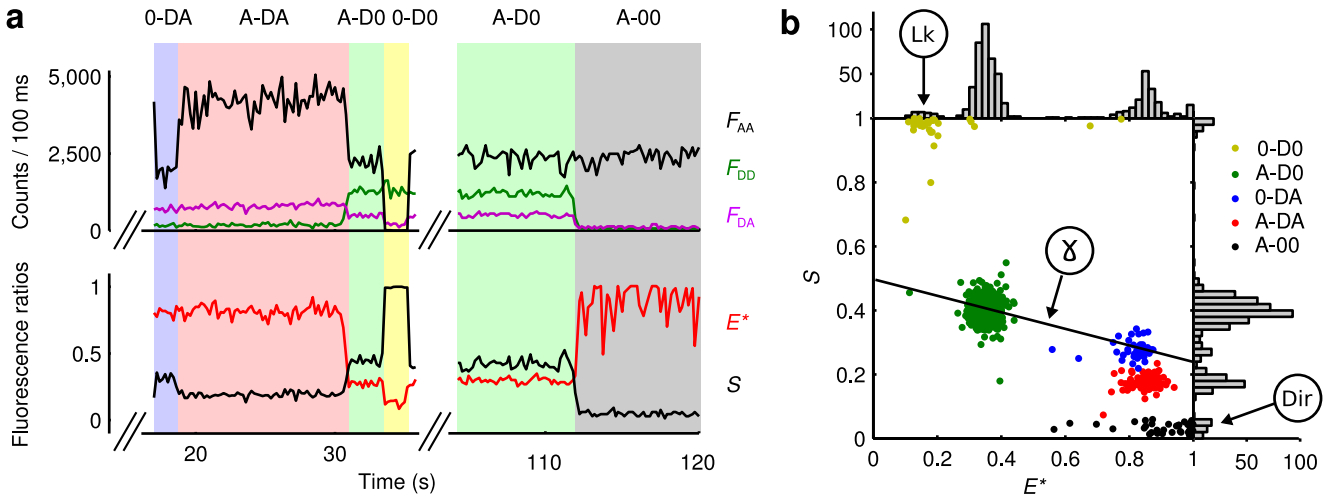

Supplementary Figure 2 | Accurate FRET efficiencies from a single molecule. (**a**) Sections of an ALEX time-trace from Cy5-Cy3B-Cy5 experiments. In addition to the four states (0-D0, A-D0, 0-DA, A-DA) discussed in **Fig. 2**, this time-trace also shows an acceptor-only state (A-00) after the donor bleached (grey background). (**b**) The presence of the clusters 0-D0, A-D0, 0-DA, and A-00 in the E^*-S histogram allows the calculation of accurate FRET efficiencies E. The donor-only state 0-D0 gives information on the leakage factor Lk. The acceptor-only state A-00 is used to estimate the acceptor-direct-excitation factor Dir. The slope between A-D0 and 0-DA after correction for direct excitation and leakage yields the detection correction factor γ, which is used for calculating accurate FRET efficiencies.

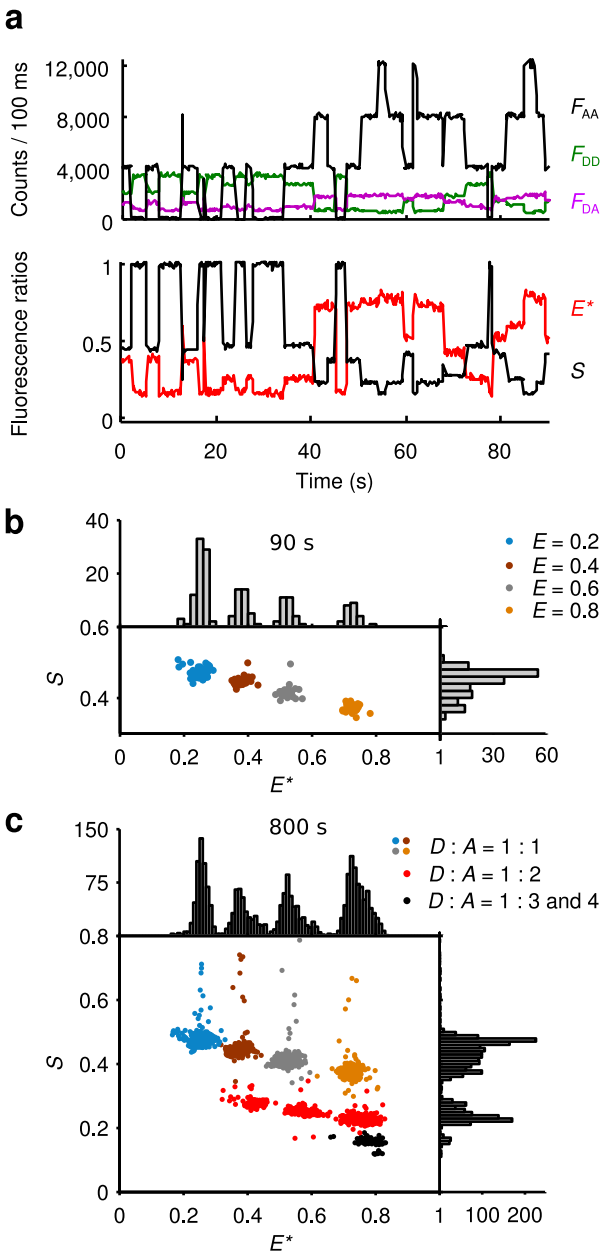

Supplementary Figure 3 | Monte Carlo simulation of switchable FRET with four acceptors. (**a**) Simulated ALEX time-trace of a system with one donor and four acceptors with individual FRET efficiencies of $E = 0.2$, 0.4, 0.6, and 0.8, respectively. The simulation parameters reflected the photophysical properties of Cy3B and Cy5 (see **Supplementary Table 4**). (**b**) E^*-S histogram of the four single-pair FRET states of the data in **a**. The E^* values differ from the input E values because of the simulated donor leakage and the effect of γ, which also causes the negative slope between the clusters. (**c**) The E^*-S histogram of a simulated time-trace of 800 s displays the four individual FRET states at intermediate S (D:A = 1:1). At lower S, there are six partly overlapping clusters with two active acceptors (D:A = 1:2), four overlapping clusters with three active acceptors (D:A = 1:3), and a few data points with four active acceptors (D:A = 1:4, at lowest S). The donor-only state was omitted for clarity.

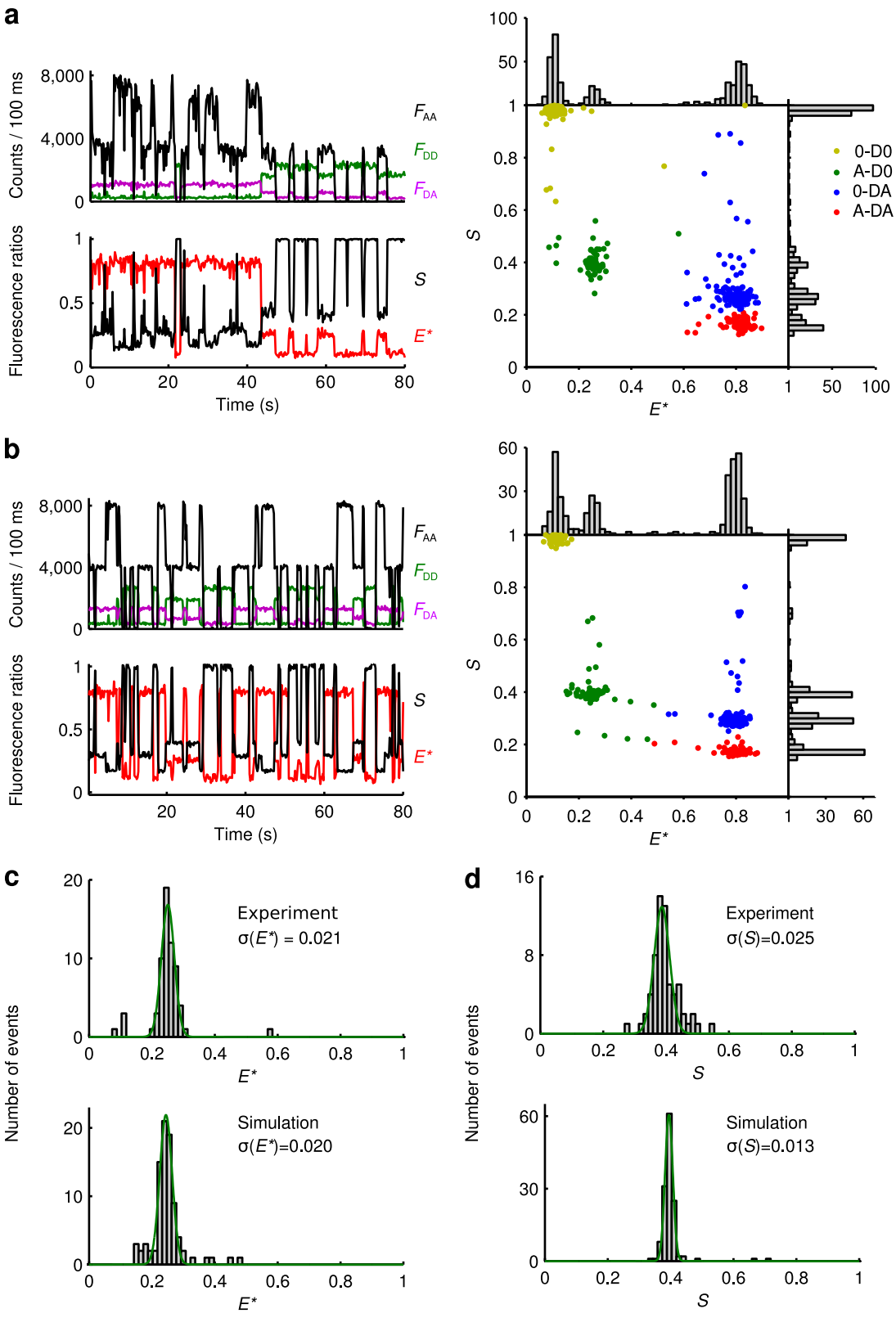

Supplementary Figure 4 | Direct comparison between simulation and Cy5-Cy3B-Cy5 experiment. (**a**) Experimental ALEX time-trace and E^*-S histogram from **Fig. 2**. (**b**) Simulated ALEX time-trace and E^*-S histogram (for simulation parameters see **Supplementary Table 4**). (**c**) Experimental (top) and simulated (bottom) FRET distributions of the cluster A-D0 from the data in **a,b**. The standard deviation was obtained from a Gaussian fit. (**d**) Stoichiometry distributions for cluster A-D0.

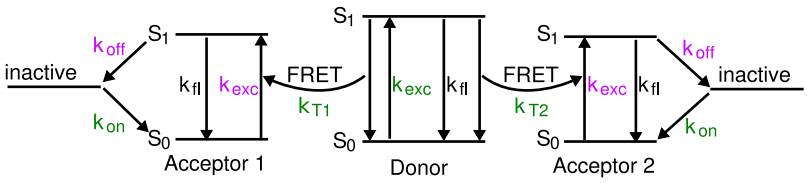

Supplementary Figure 5 | Energy diagram and model for switchable FRET with one donor and two acceptors (for simulation parameters see **Supplementary Table 4**). Each fluorophore cycles between its ground state S_0 and excited state S_1 by excitation (k_{exc}) and fluorescence emission (k_{fl}). The donor transfers energy to either acceptor via FRET (k_{T}). The acceptors switch-off by a transition to an inactive state (k_{off}) and switch-on by a transition to the ground state (k_{on}). Green and red excitation dependent rates are highlighted in color.

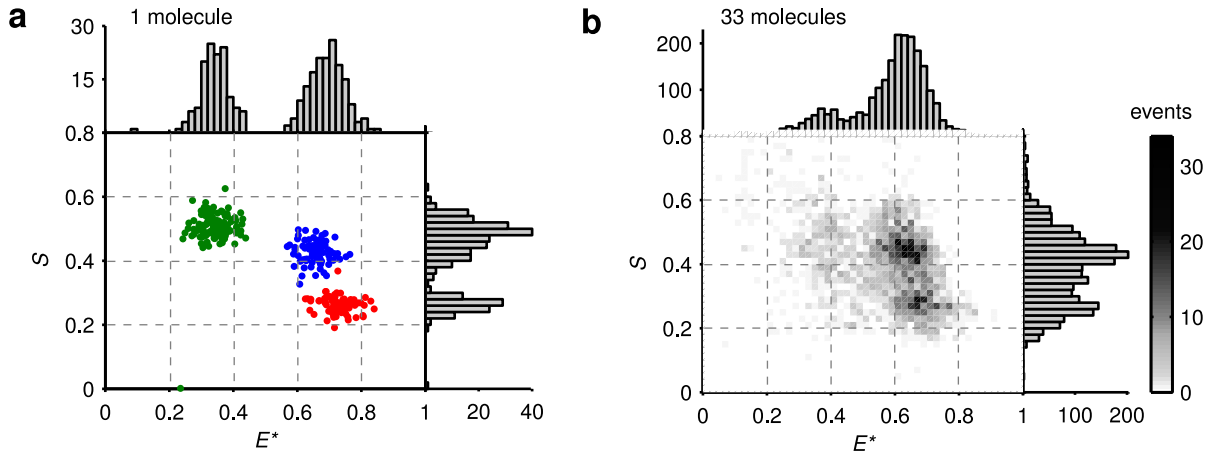

Supplementary Figure 6 | Single-molecule vs. combined E^*-S histogram for the CAP-DNA complex. (**a,b**) Single-molecule data from **Fig. 4** compared to the combined data of 33 molecules measured under identical conditions. Increased heterogeneity between different molecules within the CAP-DNA sample compared to the Cy5-Cy3B-Cy5 sample (**Supplementary Figure 1**) is apparent from the increased width of clusters, most likely representing the distribution of DNA bend angles within the sample.

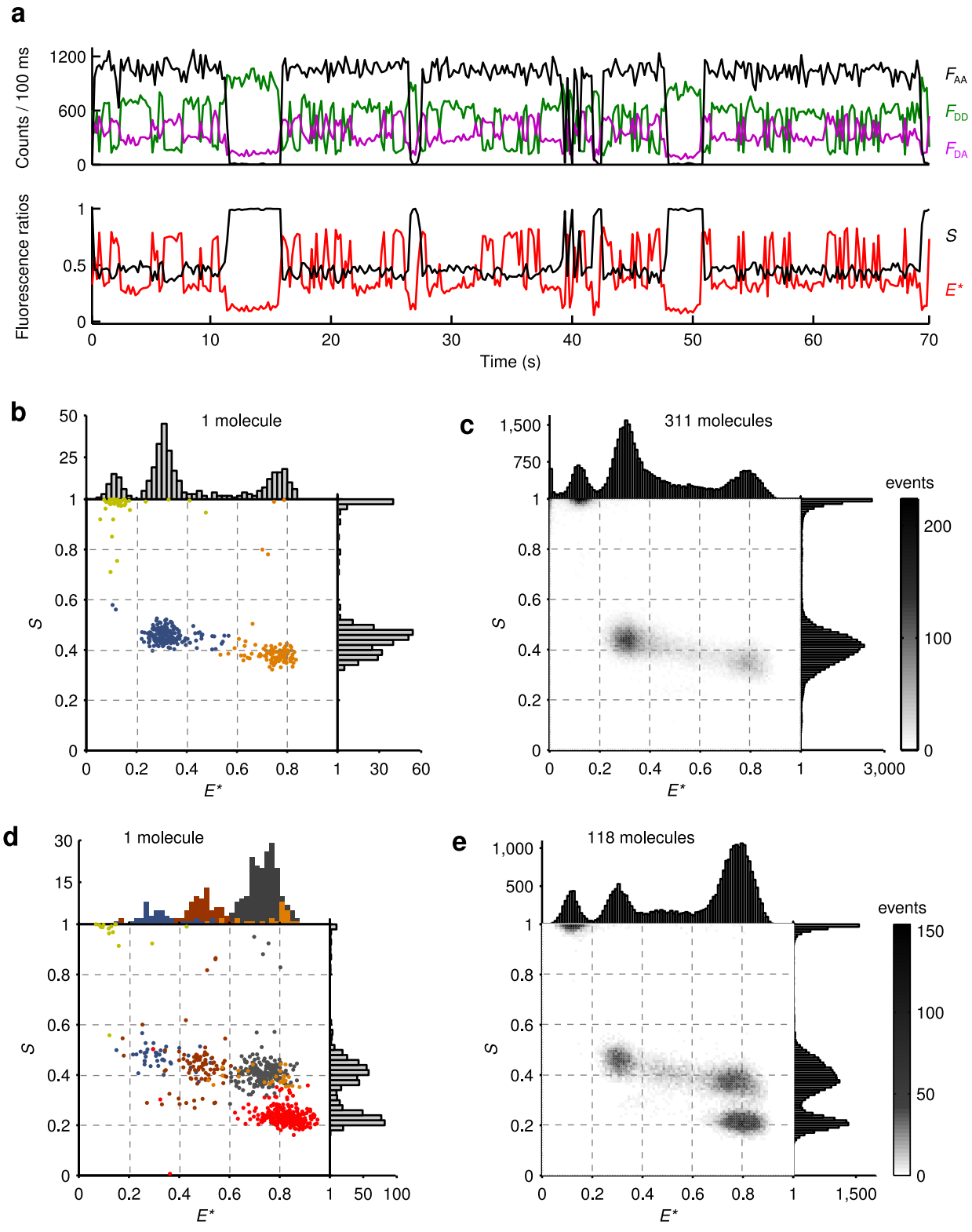

Supplementary Figure 7 | Holliday junction controls. (**a**) ALEX time-trace showing dynamics of a single Holliday junction from a control sample labeled with e-Cy5 and Cy3B only. (**b**) E^*-S histogram of the data in **a**. (**c**) Combined E^*-S histogram of 311 molecules of the control sample measured under identical conditions. (**d,e**) Single-molecule data from **Fig. 5f** compared to the combined data of 118 molecules that showed conformational dynamics.

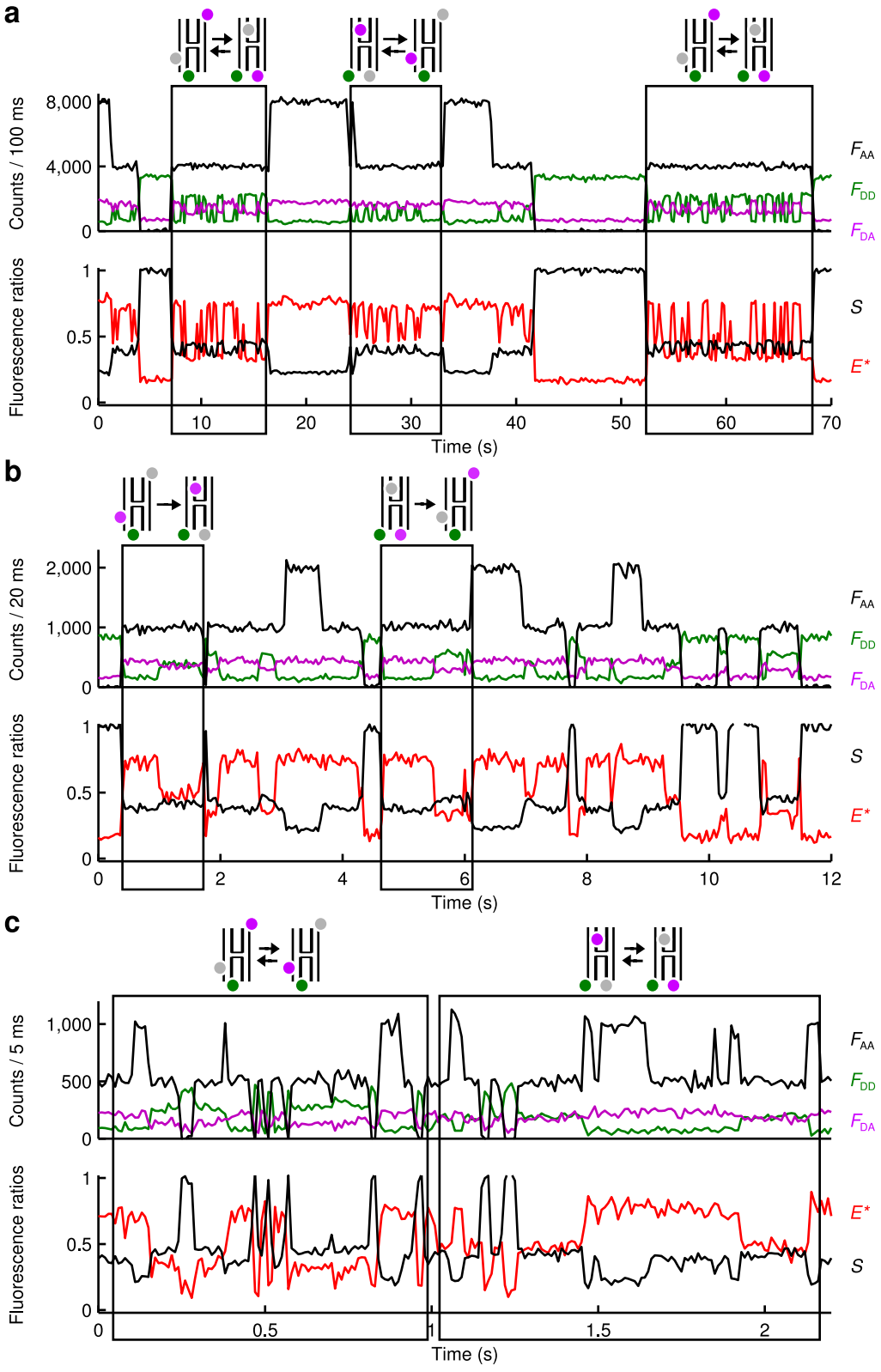

Supplementary Figure 8 | Simulation of Holliday junction dynamics with switchable FRET. (**a**) Slow photoswitching compared to dynamic rates. Boxed sections display a single acceptor probing multiple conformational changes (at 200 ms temporal resolution). (**b**) Similar photoswitching and dynamic rates. Boxed sections display a single acceptor probing individual conformational changes (at 40 ms temporal resolution). (**c**) Fast photoswitching compared to dynamic rates. Boxed sections display a single conformational state probed multiple times by two acceptors (at 10 ms temporal resolution). Simulation parameters are given in **Supplementary Table 4**.

Cy5-Cy3B-Cy5 Construct	
Top Strand	5'-CAG ACG GCT GGC ACG ACT TXT GCA CGA TCA GCC CTG GGC GAG CGC ATT GTT GCG C-Biotin, modified at the 3'-end with Biotin and at position 20 (X) with Cy3B.
Bottom Strand	5'-GCG CAA CAA TGC GCT CGC CCA GGG CYG ATC GTG CAA AAG TCG TGC CAG CCG TCT G-Cy5, modified at the 3'-end and at position 30 (Y) with Cy5.
Cy5-Cy3B Control: Identical to Cy5-Cy3B-Cy5 construct, except that the bottom strand is only 3'-modified with Cy5.	
Cy3B-Cy5 Control: Identical to Cy5-Cy3B-Cy5 construct, except that the bottom strand is only modified at position 30 with Cy5.	
ATTO655-Cy3B-ATTO655 Construct	
Top Strand	5'-AAG ACG GCT GGC ACG ACT TXT GCA CGG TAA ATG CTG GGC GAG CGC ATT GTT GCG C-Biotin, modified at the 3'-end with Biotin and at position 20 (X) with Cy3B.
Bottom Strand	5'-GCG CAA CAA TGC GCT CGC CCA GCA TYT ACC GTG CAA AAG TCG TGC CAG CCG TCT T-ATTO655, modified at the 3'-end and at position 30 (Y) with ATTO655.
ICAP DNA Construct	
Top Strand	5'-Cy3B-AAC GCA ATA AAT GTG AAG TAG ATC ACA TTT TAG GCA CCA, modified at the 5'-end with Cy3B.
Bottom Strand	5'-Biotin-TGG TGC CTA AAA TGT GAT CTA CTT CAC ATT TAT TGC GTT, modified with Biotin at the 5'-end.
Holliday junction Constructs	
X Strand	Cy3B-5'-CCC AGT TGA GAG CTT GAT AGG G, modified at the 5'-end with Cy3B.
B Strand	5'-CCC TAX CAA GCC GCT GCT ACG G, modified at position 6 (X) with Cy5 (internal "i-Cy5").
R Strand	Cy5-5'-CCC ACC GCT CTT CTC AAC TGG G, modified at the 5'-end with Cy5 (end "e-Cy5").
H Strand	Biotin-5'-CCG TAG CAG CGA GAG CGG TGG G, modified at the 5'-end with Biotin.

Supplementary Table 1 | DNA sequences (5'-3') and modifications.

Experiment	5 states	4 states	3 states	2 states	1 state	ambiguous
Cy5-Cy3B-Cy5	-	57%	28%	6%	0%	9%
ATTO655-Cy3B-ATTO655	-	48%	13%	8%	0%	31%
CAP-DNA	-	26%	48%	9%	0%	17%
Holliday junction	8%	42%	22%	20%	2%	6%

Supplementary Table 2 | Percentages of molecules of the different experiments that exhibited a certain number of states. To account for incomplete labelling, only fully labeled molecules that carried two acceptors and a donor were included by filtering all recorded particles based on emission intensity thresholds and the presence of dual-step photobleaching/photoswitching events in the F_{AA} time-trace. Molecules marked "ambiguous" showed no clear states or states at unexpected positions.

Cluster	0-D0	A-D0	0-DA	A-DA
E^*	0.113 ± 0.005	0.279 ± 0.001	0.778 ± 0.006	0.811 ± 0.003
S	0.970 ± 0.001	0.394 ± 0.002	0.264 ± 0.003	0.168 ± 0.002
E_{PR}	-0.001 ± 0.008	0.174 ± 0.005	0.729 ± 0.008	0.751 ± 0.009
E	-0.001 ± 0.023	0.386 ± 0.008	0.889 ± 0.004	0.900 ± 0.004
E_{th}	0	0.387	0.890	0.896 ± 0.004

Supplementary Table 3 | Accurate FRET data for molecule in **Supplementary Fig. 2**. Whereas acceptor-direct-excitation Dir has a minor effect ($Dir = 0.036 \pm 0.002$), the leakage is substantial with about 13% of the donor emission being detected in the acceptor channel ($Lk = 0.127 \pm 0.002$). Correction of leakage and direct excitation yields the FRET proximity ratio E_{PR}. Because of the distinct slope between A-D0 and 0-DA in the E^*-S histogram, the effect of $\gamma = 0.336 \pm 0.001$ must be corrected for, yielding accurate FRET efficiencies E. Here, E^* is closer to E than E_{PR} because the effects of leakage and γ partially cancel out. Standard errors of the mean (s.e.m.) were calculated by error propagation of the s.e.m. of the clusters in the E^*-S histogram. Theoretical FRET E_{th} for A-D0 and 0-DA was calculated from equations 7 and 8 (**Online Methods**) assuming a cylindrical model of helical DNA. Applying theory of FRET between one donor and multiple acceptors, theoretical E_{th} of A-DA was calculated based on the measured E of A-D0 and 0-DA (equation 9, **Online Methods**).

Fig.	4	Suppl. 3	Suppl. 8a	Suppl. 8b	Suppl. 8c
E_1	0.2	0.284	0.333, 0.821	0.333, 0.821	0.333, 0.821
E_2	0.4	0.872	0.798, 0.539	0.798, 0.539	0.798, 0.539
E_3	0.6	-	-	-	-
E_4	0.8	-	-	-	-
k_{on}	0.32	1.6	0.3	3	30
k_{off}	0.2	0.4	0.1	1	10
$k_{\mathrm{I\text{-}II}}$	-	-	2	2	0.2
$k_{\mathrm{II\text{-}I}}$	-	-	3	3	0.3
Exposure time	0.1	0.1	0.1	0.02	0.005
$F_{\mathrm{DD}} + F_{\mathrm{DA}}$	4000	3000	4000	1000	500
F_{AA}	4000	4000	4000	1000	500
B_{DD}	30	30	31	6	3
B_{DA}	34	34	31	6	3
B_{AA}	38	38	31	6	3
γ	0.5	0.481	0.5	0.5	0.5
Lk	0.2	0.129	0.2	0.2	0.2

Supplementary Table 4 | Simulation parameters. E_1-E_4: Accurate FRET efficiencies for each acceptor. In **Supplementary Fig. 8**, each acceptor has two values corresponding to two interconverting conformations. k_{on}, k_{off}: Photoswitching rates $\left(s^{-1}\right)$. $k_{\mathrm{I\text{-}II}}$, $k_{\mathrm{II\text{-}I}}$: Dynamic rates $\left(s^{-1}\right)$. Exposure time (s). $F_{\mathrm{DD}} + F_{\mathrm{DA}}$, F_{AA}: Emission intensities (counts/(exposure)). B_{DD}, B_{DA}, B_{AA}: Background intensities (counts/(pixel $\cdot$ exposure)). γ, Lk: Detection biases and leakage.